Green Chemistry

PAPER

View Article Online
View Journal | View Issue

Cite this: *Green Chem.*, 2024, **26**, 3949

Direct amination of poly(*p*-phenylene oxide) to substituted anilines over bimetallic Pd–Ru catalysts†

Phuc T. T. Nguyen, ‡[a,b] Gökalp Gözaydın,‡[a] Jieran Ma,[a] Bingqing Yao,[c] Qian He [c] and Ning Yan *[a,b]

Received 5th October 2023,
Accepted 28th January 2024

DOI: 10.1039/d3gc03757f

rsc.li/greenchem

Chemical upcycling of plastic waste offers a promising opportunity for synthesizing value-added products. Despite its potential, transforming poly(phenylene oxide) (PPO) into nitrogen-based chemicals remains underexplored. To that end, we report the direct conversion of PPO to dimethylanilines over bimetallic Pd–Ru/CNT in a mixture of octane and aqueous ammonia. In a one-pot manner, PPO is initially converted into substituted phenols, and then is aminated, yielding 30% dimethylanilines over Pd_7Ru_3/CNT under optimum conditions. The bimetallic catalyst outperforms its monometallic equivalents. Transmission electron microscopy (TEM), powder X-ray diffraction (XRD) and energy-dispersive X-ray spectroscopy (EDX) unveiled the features of well dispersed and small-sized metallic nanoparticles. Control experiments using deuterium indicated a high reliance of hydrogen and water for the amination step and the hydrogenolysis step, respectively. Furthermore, we demonstrated product isolation through a straightforward acid–base treatment and extraction. This work introduces a viable route for upcycling PPO into valuable nitrogen-containing compounds.

Introduction

Plastic production has grown rapidly since the middle of the last century. However, the generation of plastic waste is an alarming problem, with less than 10% of plastic waste being recycled.[1] While mechanical recycling is the dominant pathway at present, it often leads to the formation of lower-value products due to the deterioration of virgin properties through successive processes.[2] Chemical recycling is an alternative approach, generating small molecular compounds from plastic that could either be repolymerized or directly used as fine chemicals.[3,4] Current research focuses on the catalytic activation of C–C, C–O, and C–N bonds in common plastics, leading to the formation of various chemicals such as aliphatic hydrocarbons,[5–19] arenes[20–23] and oxygenates.[24–26]

Organonitrogen chemicals, constituting over 80% of the top 200 pharmaceuticals among others, are pivotal in the chemical sector.[27] To foster green chemistry, there's a push to derive these chemicals from non-fossil resources like waste polymers.[28] Ammonolysis and aminolysis techniques have been explored to convert polyethylene terephthalate[29–35] and certain polyamides[36–38] to amines and amides. Additionally, alanine was efficiently produced from biodegradable polylactic acid using ammonia and Ru/TiO_2, with impressive purity and selectivity obtained over multiple cycles.[39] More recently, lignin as an aromatic polymer has been converted into phenolic amines using Ru catalyst,[40] emphasizing the potential of making amines from aromatic polymers.

Poly(*p*-phenylene oxide) (PPO) is a versatile engineering plastic exhibiting high heat resistance and stability. It is made *via* the oxidative condensation of 2,6-dimethylphenol, and it is broadly used spanning from electronics to automotive production. Despite its USD 1.67 billion market size in 2019, the catalytic conversion of PPO into other valuable chemicals has not been thoroughly studied.[41] Notably, Ru/Nb_2O_5 has been identified for its ability to cleave PPO's C–O bonds. By adjusting the metal particle size, distinct products like *m*-xylene or 3,5-dimethylphenol have been selectively obtained.[42,43] Small-sized metal particles are responsible for preserving the phenolic hydroxyl group while Brønsted acid sites facilitate the cleavage of C(o)–O bonds rather than C(m)–O bonds.

[a]*Department of Chemical and Biomolecular Engineering, National University of Singapore, 4 Engineering Drive 4, 117585, Singapore. E-mail: ning.yan@nus.edu.sg*
[b]*Joint School of National University of Singapore and Tianjin University, Fuzhou 350207, Fujian, China*
[c]*Department of Materials Science and Engineering, National University of Singapore, Singapore 117575, Singapore*

†Electronic supplementary information (ESI) available: TEM images, particle size distribution, STEM image, elemental maps, product yield and gas phase analysis of PPO hydrogenolysis to dimethylphenols using deuterium, MS spectra. See DOI: https://doi.org/10.1039/d3gc03757f

‡Both authors contributed equally to this work.

Dimethylanilines are essential for producing dyes and pharmaceuticals.[44] They are commercially produced by the amination of substituted phenols in the presence of aluminum oxide-containing catalysts, aluminum salt as well as hydrogen transfer catalyst with cyclohexanone co-catalyst.[45–48] The market size of 2,6-dimethylaniline and 3,5-dimethylaniline reached USD 50 million[49] and USD 33 million[50] in 2022, respectively. Considering the structural similarity between PPO unit and dimethylanilines, and the established methods for the catalytic conversion of phenolic compounds to anilines,[51–55] one-pot catalytic system for the transformation PPO to dimethylanilines using metal catalyst was explored in this study. Transforming PPO to dimethylanilines involves two primary steps: PPO's hydrogenolysis to dimethylphenols (either 3,5 or 2,6 substitution) and the subsequent amination of dimethylphenols to dimethylanilines. The latter step requires the partial hydrogenation of dimethylphenols into dimethylcyclohexanones, followed by imination and a series of hydrogenation/dehydrogenation reactions to produce dimethylanilines. Given the known dehydrogenation properties of the Pd-based catalyst for the cyclohexane ring,[56,57] Pd was chosen as an active component. Meanwhile, Ru on carbon nanotubes (CNT) is recognized for its efficiency in amination reactions,[58,59] due to its enhancement of alcohol dehydrogenation in the presence of NH_3, its ability to hydrogenolyze Schiff bases to primary amines, and the stability of CNT as the catalyst support under highly basic conditions.[60] This knowledge led us to consider a nanoalloy Pd–Ru/CNT catalyst for the one-pot PPO to dimethylanilines transformation (Scheme 1).

Experimental

Materials

PPO (98%, M_w 40 000–50 000) was purchased from BLDpharm. $Pd(NO_3)_2{\cdot}2H_2O$ (40% Pd basis), $RuCl_3{\cdot}xH_2O$ (40.00–49.00% Ru basic), 2,6-dimethylphenol (99%), 3,5-dimethylphenol (99%), 2,6-dimethylaniline (99%), 3,5-dimethylaniline (98%), octane (98%), toluene (anhydrous, 99.8%), 2-methyltetrahydrofuran (2-MeTHF, 99.5%), *tert*-amyl alcohol (TAA, 99%) were purchased from Sigma Aldrich. Aqueous ammonia solution (25%) and ethyl acetate (≥99.5%) were purchased from VWR. CNT (multiwalled carbon nanotube) was purchased from ANR Technologies.

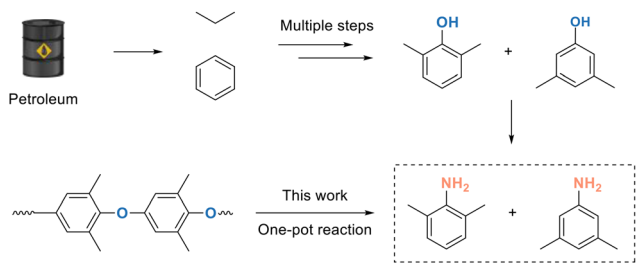

Scheme 1 Conventional pathway to dimethylanilines from petroleum and our approach.

Catalyst preparation

The CNT-supported bimetallic catalysts with a Pd to Ru weight ratio of $x:y$ (denoted as Pd_xRu_y/CNT) were synthesized by incipient wetness impregnation using $Pd(NO_3)_2{\cdot}2H_2O$ and $RuCl_3{\cdot}xH_2O$ as the precursors. Under this terminology, 2% Pd_7Ru_3/CNT refers to bimetallic PdRu catalyst, with a total metal loading of 2 weight percentage, and a Pd : Ru weight ratio of 7 : 3. Typically, CNT was washed with a 5 M HCl aqueous solution (30 mL g^{-1}) for 4 h, filtrated, rinsed with water (3 L g^{-1}) to remove metal impurities and dried at 100 °C for 12 h before use. $Pd(NO_3)_2{\cdot}2H_2O$ and $RuCl_3{\cdot}xH_2O$ were dissolved in 2 mL water by sonicating for 30 min and mixed with 0.5 g CNT. After being dried at 100 °C for 12 h, the catalyst was reduced at 400 °C under 5% H_2/N_2 for 2 h. Pd–Ru loaded on other supports (ZrO_2, TiO_2, CeO_2, and MgO) catalysts were prepared with the same incipient wetness impregnation method.

Catalyst characterization

Transmission electron microscopy (TEM) analysis was performed using a JEM 2100F (JEOL, Japan) and a JEM 2800 (JEOL, Japan) at 200 kV using the sample placed on a Formvar-coated copper grid. Powder X-ray diffraction (XRD) spectra were obtained on a Bruker D8 Advance machine over a scan rate of 0.05°s^{-1}. Raman spectra were obtained by a Raman microscope (XploRATM Plus, HORIBA Scientific) with a 638 nm excitation laser. Scanning transmission electron microscopy (STEM) and energy-dispersive X-ray spectroscopy (EDX) were performed using a JEM 2800 (JEOL) at 200 kV.

Catalyst activity evaluation

Amination of PPO was performed in a 20 mL autoclave with a magnetic stirrer. Typically, PPO (50 mg), catalyst (50 mg), solvent (4 mL) and 25% aqueous ammonia solution (1 mL) were added. The autoclave was sealed and purged with N_2 and H_2 several times. Afterwards, the H_2 pressure was adjusted to the desired value and the autoclave was placed into a pre-heated steel holder, which was heated by a hot plate and insulated by a jacket. After a certain period of reaction at the desired temperature, the autoclave was cooled down in an ice-water bath. The catalyst was separated from the liquid through filtration using a PTFE syringe filter (0.45 μm) and ethyl acetate (~15 mL). Quantitative and qualitative analysis of the liquid product was performed using a gas chromatography – flame ionization detection (GC-FID, Agilent GC 7890A) and a gas chromatography – mass spectrometry (GC-MS, Agilent 7890A GC system and 5975C inert MSD with a triple-axis detector) equipped with an HP-5 column. GC samples were prepared by mixing the reaction sample and 100 μL internal standard solution (pentadecane in octane, 0.1 g mL^{-1}). GC-FID oven program was set to initial temperature of 60 °C, heat at 5 °C min^{-1} until 150 °C (hold 3 min), heat at 1 °C min^{-1} until 180 °C (hold 3 min), and heat at 15 °C min^{-1} until 300 °C (hold 4 min). A similar oven program was used for the GC-MS.

The Pd and Ru contents in the reaction mixture were determined using inductively coupled plasma optical emission spectroscopy (ICP-OES) on a Thermo Scientific iCAP 6000 series ICP spectrometer. For some experiments with D_2, the gas phase (H_2, HD, D_2) was analyzed using a Hiden Analytical HPR–20 R&D quadrupole mass spectrometer.

For the recycling test, the catalyst was separated from the reaction mixture by centrifugation. The liquid phase underwent quantitative analysis using GC, while the solid catalyst was sonicated with 6 mL of toluene for 1 hour to dissolve any unreacted PPO. Following this, the catalyst was washed with 15 mL of ethanol and was subsequently dried in an oven at 60 °C for 12 hours before either direct use in the subsequent run or being sent for characterization. Starting from the second cycle, due to some catalyst loss after treatment, the amount of PPO was adjusted based on the remaining catalyst to maintain a consistent PPO : catalyst mass ratio.

Results and discussion

The bimetallic catalysts on CNT were prepared *via* the incipient wetness impregnation method (Fig. 1a). The structure of 2% Pd_7Ru_3/CNT is evidenced by STEM (Fig. 1b), showing metallic nanoparticles of about 2.4 nm in size (Fig. 1c) on CNT. The size of the nanoparticles is in between the sizes of the two monometallic equivalents. Specifically, 2% Pd/CNT had a larger average size of 4.3 nm, whereas 2% Ru/CNT was smaller at 1.3 nm (Fig. S1†). Some large particles over 10 nm were seen in 2% Pd/CNT. Consistent with this, XRD analysis (Fig. 1d) showed only Pd/CNT had clear metal particle crystal phases. Elemental mapping (Fig. 1c) depicted an even distribution of Pd and Ru on the support. Further inspection (Fig. S2†) suggested Pd and Ru co-existence within particles. These observations affirm the fine dispersion and small size of Pd and Ru in the 2% loading bimetallic catalyst. Raman spectroscopy was used to study CNT structure differences among the catalysts (Fig. 1e). Characteristic CNT peaks at 1321 cm^{-1}, 1606 cm^{-1}, 1580 cm^{-1}, and 2641 cm^{-1} were identified.[61] Metal doping leads to a subtle I_D/I_G intensity ratio decrease from 1.73 to 1.46–1.62, indicating possible defect annealing during 400 °C catalyst reduction.[62] Bimetallic catalysts supported on CNT with varying Pd : Ru weight ratios (0 : 1, 3 : 7, 5 : 5, 7 : 3, 1 : 0) were synthesized and evaluated for PPO conversion to dimethylanilines at 5 bar H_2, 280 °C for 4 h. Pd/CNT achieved a 3% dimethylanilines yield, while Ru/CNT was inactive for amination. The Pd_7Ru_3/CNT bimetallic catalyst significantly improved the dimethylanilines yield to 21.1% in an octane and aqueous ammonia mixture solvent (Fig. 2a). As temperatures increased, dimethylanilines yield followed a volcano trend, while dimethylphenols yield consistently increased to 36.3% (Fig. 2b). At 260 °C, hydrogenated products prevailed due to the exothermic hydrogenation of aromatic rings (low temperature favoured).[55,63] H_2 pressure also exhibited a volcano type of trend (Fig. 2c): at 1 bar H_2 atmosphere, hydrogenolysis and amination did not occur, while 10 bar H_2 led to benzene ring hydrogenation, producing nearly 90% reduced products. Previous studies indicate that aromatic compound formation from plastic and biomass depends on catalyst nanoparticle size, with smaller sizes preferred to prevent benzene ring hydrogenation and adsorption.[42,43,64] Thus, we assessed how the metal loading of Pd_7Ru_3/CNT impacts PPO amination (Fig. 2d). The yields of dimethylanilines and dimethylphenols tended to rise as metal loading decreased from 10% (3.2 nm, Fig. S3†) to 2% (2.4 nm, Fig. S3†), reaching a 30.4% amine yield. Conversely, *m*-xylene yield fell from 33.6% to 10.1%. At a further reduced metal loading of 0.5%, 6% phenolic monomers emerged due to limited metal sites for hydrogenolysis. Recognizing that a 2% metal loading is optimal, we evaluated the performance of 2% Pd_7Ru_3 on various supports (Fig. S4†). Besides Pd_7Ru_3/CNT, only the MgO-supported catalyst exhibited moderate activity, yielding 19.3% of dimethylanilines. In contrast, Pd_7Ru_3 supported on ZrO_2, TiO_2, and CeO_2 was found to be inactive.[58]

Interestingly, the catalyst was active only with an octane-ammonia mixture (Fig. 2e). While toluene and TAA were effective for lignin amination,[65] they yielded minimal monomers from PPO. The distinctive impact of octane can be explained by its capacity to facilitate PPO dispersion even at room temperature[42] (Table S1†), as well as its inert nature to the Pd_7Ru_3/CNT under the hydrogenation condition. While toluene has the capability to dissolve PPO, its poor performance is attributed to the undesired hydrogenation of toluene

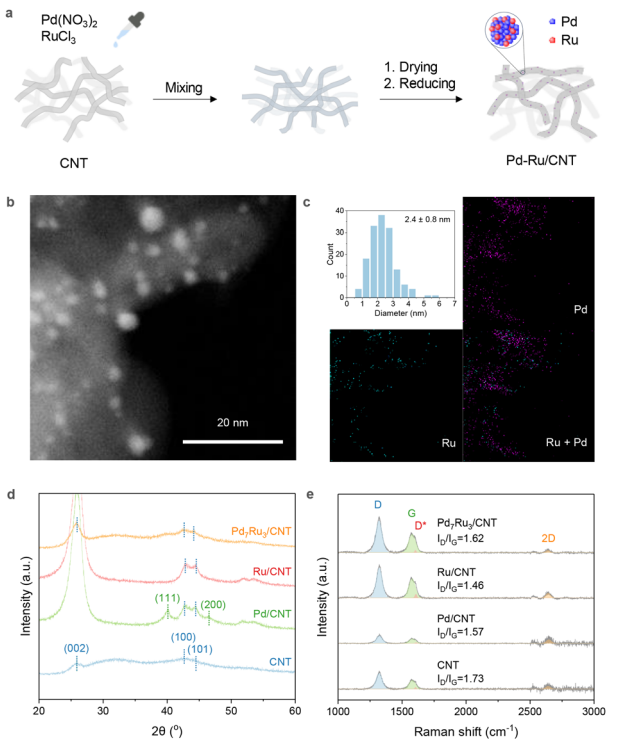

Fig. 1 (a) Schematic diagram of the 2 wt% Pd_7Ru_3/CNT preparation method, (b) STEM image of 2 wt% Pd_7Ru_3/CNT, (c) particle size distribution and elemental mapping of 2 wt% Pd_7Ru_3/CNT. (d) XRD analysis and (e) Raman spectra of CNT and the catalysts at 2% metal loading.

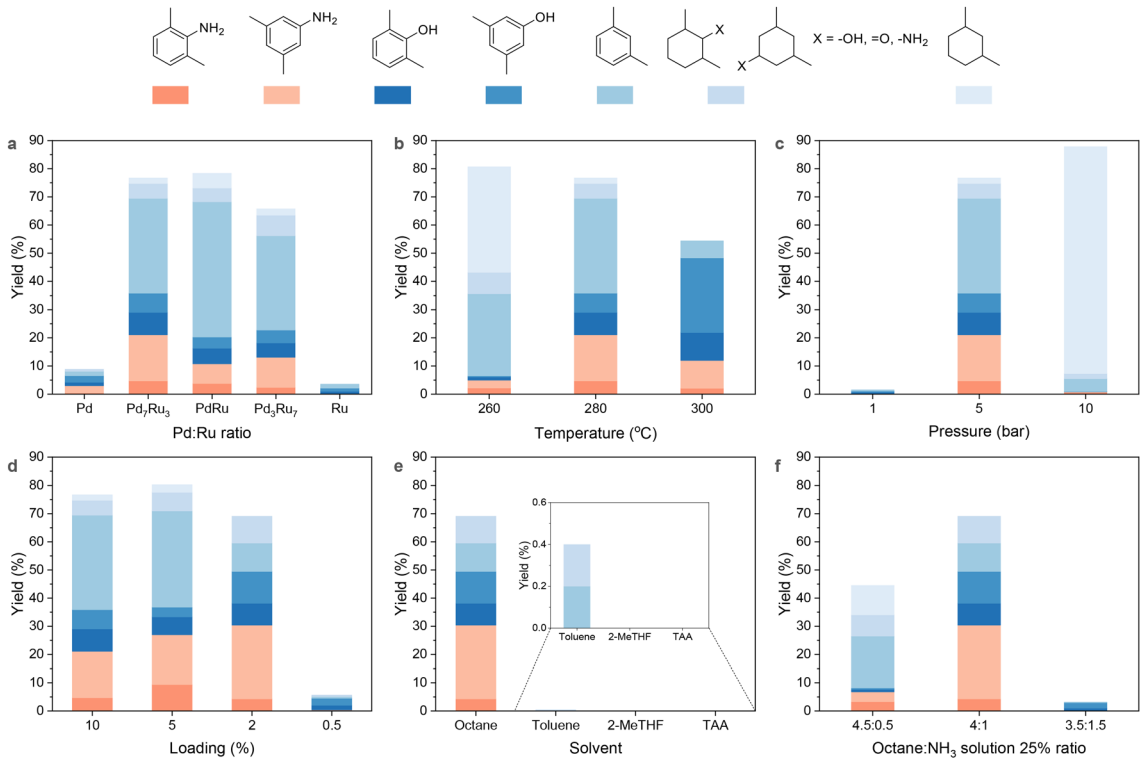

Fig. 2 The influence of conditions for the conversion of PPO over bimetallic Pd–Ru/CNT catalyst: (a) Pd : Ru weight ratio, (b) reaction temperature, (c) H_2 pressure, (d) metal loading, (e) solvent type, and (f) octane to 25% aqueous NH_3 aqueous solution ratio. Reaction condition: 50 mg PPO, 50 mg catalyst, 4 mL octane, 1 mL 25% aqueous NH_3 solution, 5 bar H_2, 280 °C, 4 h. Catalyst: (a) 10% metal/CNT, (b and c) 10% Pd_7Ru_3/CNT, (d) Pd_7Ru_3/CNT, (e and f) 2% Pd_7Ru_3/CNT. For (f), the total volume of solvent was maintained at 5 mL. 2-MeTHF: 2-methyltetrahydrofuran, TAA: *tert*-amyl alcohol.

to methylcyclohexane, which occupies the catalytic sites and consumes hydrogen (Fig. S5†). Moreover, aromatic amine production from PPO was sensitive to the octane-NH_3 ratio (Fig. 2f). Change in ammonia amount dramatically affected the dimethylaniline yield, with the best ratio between octane to ammonia at 4 : 1 being identified. A lower ratio resulted in the aggregation of PPO and the catalyst (Fig. S6†), hindering the depolymerization of PPO.

We assessed the effect of D_2 in PPO amination using 2% Pd_7Ru_3/CNT by substituting H_2 with D_2. Three trials were performed: direct PPO conversion to amines (one-pot), PPO hydrogenolysis without NH_3 (step 1), and substituted dimethylphenol amination (step 2), with results shown in Fig. 3. Switching to D_2 (Fig. 3a) led to reduced dimethylamines yields in the one-pot reaction (13.9%) and step 2 (12.5%) but left dimethylphenols yields in step 1 slightly increased, suggesting amination is more hydrogen-reliant than hydrogenolysis. In contrast, replacing H_2O by D_2O resulted in a significant drop of dimethylphenols yield in step 1 to 10.0% (Fig. S7†). This highlighted D_2O is involved in the rate-limiting step in hydrogenolysis, likely occur *via* a previously reported route of water participated C–O bond breakage.[66,67] Nonetheless, the D_2-H_2 exchange catalyzed by Pd might mitigate the isotope effect.[68,69]

Additionally, the liquid products were analyzed by GC-MS to determine deuterium atom distribution within desired compounds. Utilizing mass fragmentation patterns, we established the isotopologue distribution (Fig. 3b) by fitting the mass spectra data[70] with peak areas from extracted ion chromatograms. Deuterated products always account for over 50% of total product, with mono-deuterium (d_1) being more abundant than di-deuterium (d_2) and tri-deuterium (d_3) products. Unusual adjacent fragmentations at specific *m*/*z* value of 77 ($C_6H_5^+$), 91 ($C_7H_7^+$), 106–107 (molecular ion losing a methyl group), and 121–122 (molecular ion) in the MS spectra (Fig. S8†) highlight deuterium substitution on the benzene ring. Generally, dimethylanilines and dimethylphenols exhibited consistent isotopologue patterns, but 3,5-dimethylaniline was exceptional with roughly 27% heavier isotopologues. One explanation is that 3,5-dimethylaniline has higher reactivity in dehydrogenation and hydrogenation, leading to multiple cycles that swap original hydrogen with deuterium.

To gain further insights into the reaction pathway of the PPO-to-dimethylanilines conversion process, a kinetic study was undertaken (Fig. 4a). The yield of dimethylphenols reached its highest value (35.7%) at 2 h and was considerably reduced with prolonged reaction time, suggesting its roles as intermediates. Meanwhile, the yield of dimethylanilines exhibited a gradual increase and reached a plateau after 4 h. Interestingly, *m*-xylene yield steadily grew, reaching 32.0% after 16 h; but the yield of 3,5-dimethylphenol displayed a reversed

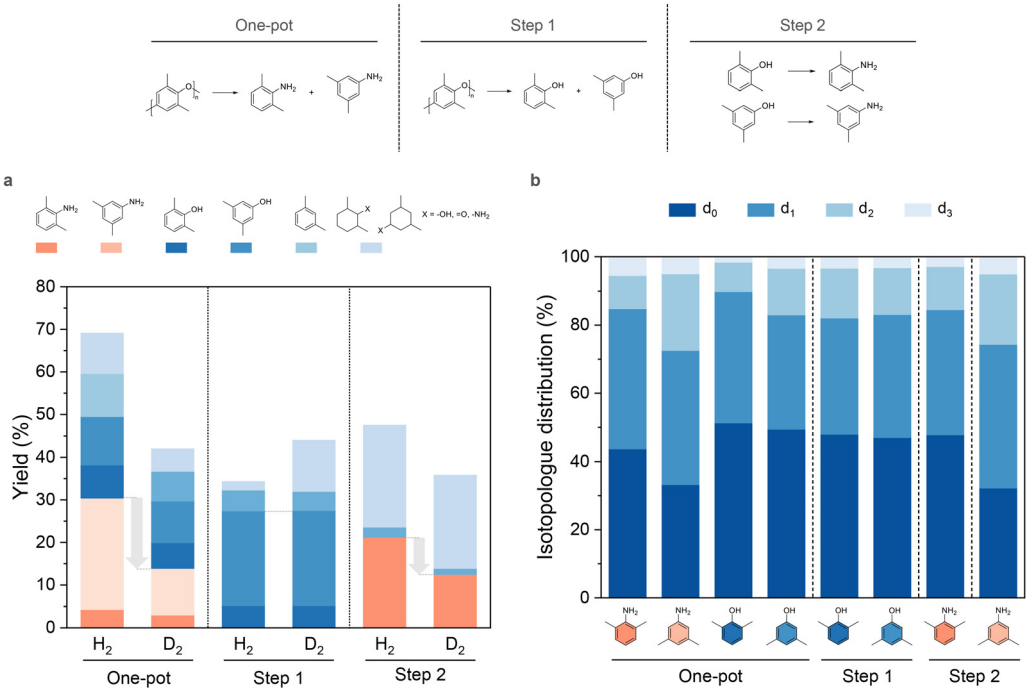

Fig. 3 (a) Product yield and (b) the distribution of deuterated and non-deuterated desired compounds. Condition for one-pot reaction (direct PPO amination): 50 mg PPO, 50 mg Pd_7Ru_3/CNT (2 wt% metal loading), 4 mL octane, 1 mL 25% NH_3 aqueous solution, 5 bar D_2 or H_2, 280 °C, 4 h. For step 1 (PPO hydrolysis to dimethylphenols), 25% aqueous NH_3 solution was replaced by water. For step 2 (dimethylphenols amination), 2,6-dimethylphenol was used in (a), and 2,6-dimethylphenol or 3,5-dimethylphenol were used in two separated experiments in (b) as starting material.

trend after 4 h. This prompted us to assess dimethylphenols and dimethylanilines' activities under the reaction condition (Fig. 4b). Regardless of -OH or -NH_2 functional groups, the 3,5-isomer, due to less steric hindrance, was less stable than the 2,6-isomer, resulting in a greater conversion. In line with the PPO amination kinetic trend, 3,5-dimethylaniline primarily became m-xylene (35.7%) within 4 h. Importantly, no isomerization was seen when using 2,6- and 3,5-isomers: 2,6-dimethylphenol didn't transform into 3,5-dimethylaniline but only produced the corresponding aniline isomers.

Based on the experimental observations, plausible reaction pathways for PPO conversion were proposed in Fig. 4c. Four main steps are involved, namely hydrogenolysis, hydrogenation, imination, and dehydrogenation. It is worth noting that although dimethylcyclohexanones are considered undesired products, they are key intermediates for the amination step. Previous research proposed that the amino group can only be incorporated into the products through the attack of ammonia on the ketone group of dimethylcyclohexanones and the resulting imines subsequently transfer hydrogen to phenol, leading to the formation of the desired anilines and the regeneration of the dimethylcyclohexanone.[71] The generation of dimethylphenols and *m*-xylene from dimethylanilines under the reaction condition suggested that this hydrogenation – imination – dehydrogenation reaction sequence is reversible. This is aligned with the proposed pathway of phenol amination over Pd/C.[72]

The by-product, *m*-xylene, is formed either through the C–O bond scissoring of dimethylphenols, or through the aromatization and hydrodeoxygenation of the reduced products.[72] It should be noted that dimer products, such as bis(3,5-dimethylphenyl)amine and 3,3′,5,5′-tetramethyl-1,1′-biphenyl, were also detected in the reaction mixture through MS analysis (Fig. S9†), indicating the occurrence of coupling reactions as side pathways.

To understand the roles of individual metal sites (Ru/Pd) and their combined effect, we examined the transformation of PPO to dimethylanilines, PPO to dimethylphenols (step 1), and 2,6-dimethylphenol to 2,6-dimethylaniline (step 2) using monometallic, bimetallic, and physically mixed catalysts (Fig. 5b–d). The GC-FID chromatograms for each route over Pd_7Ru_3/CNT are shown in Fig. 5a. In the one-pot transformation, the bimetallic catalyst surpassed both physically mixed and monometallic variants in dimethylaniline yield, following the order: Pd_7Ru_3/CNT (30.4%) > Pd/CNT (20.6%) > mixed catalyst (18.4%). This demonstrates the importance of well-dispersed and cohered active metal sites (Fig. 5b).

For step 1 (Fig. 5c), Ru/CNT demonstrated decent hydrogenolysis activity, producing 13.5% dimethylphenol yield, in line with prior studies highlighting Ru's efficacy in aromatic C–O bond cleavage in lignin.[65,73] The bimetallic catalyst showed even higher C–O linkage cleavage activity, yielding 27.4% dimethylphenols. On the other hand, step 2 (Fig. 5d) witnessed Pd/CNT outperforming Pd_7Ru_3/CNT in amination of 2,6-dimethylphenol, yielding 30.3% of 2,6-dimethylaniline. The physically mixed Ru and Pd catalysts resulted in a moderate 2,6-dimethylaniline yield (13.7%), but Ru/CNT showed no

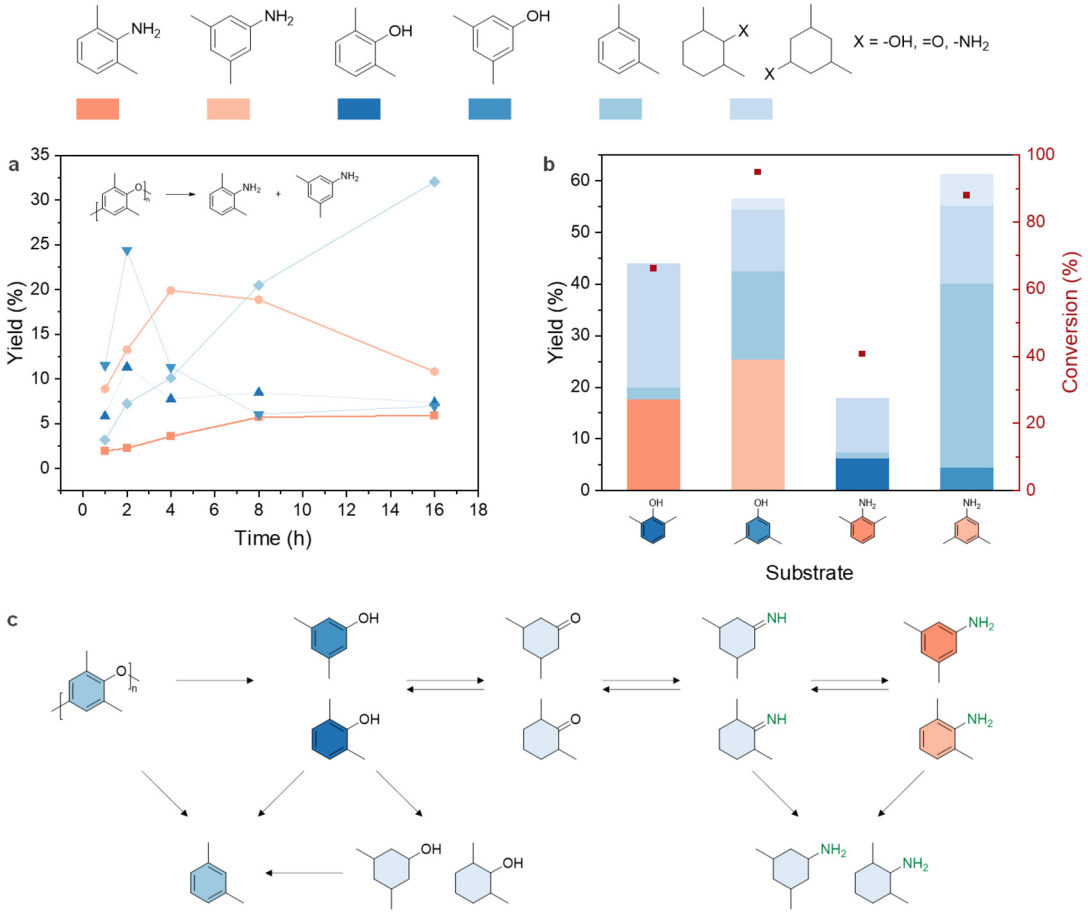

Fig. 4 (a) Kinetic study for the PPO amination, (b) reactions starting from different substrates, and (c) proposed reaction pathway. Reaction condition: 50 mg substrate, 50 mg Pd_7Ru_3/CNT (2 wt% metal loading), 4 mL octane, 1 mL 25% aqueous NH_3 solution, 5 bar H_2, 280 °C, 4 h.

activity. Pd/C's effectiveness in phenol's liquid-phase amination to aniline, in contrast with Ru/C's inertness in the step, demonstrates Pd's selectivity in the hydrogenation/dehydrogenation of aromatic rings.[52,72] Combined, these control experiments demonstrate a synergistic effect in the bimetallic catalyst in PPO amination, especially in step 1, while step 2 is predominantly Pd-dependent. Pd_7Ru_3/CNT resulted in the production of more 3,5-dimethylphenol compared to Pd/CNT and Ru/CNT, and 3,5-dimethylphenol possessed a higher activity compared to 2,6-dimethylphenol in the amination reaction (Fig. 4b). We believe that these factors induce the improved formation of dimethylanilines with Pd_7Ru_3/CNT.

Considering that dimethylanilines are generated *via* dimethylphenols amination, it might be expected that the total dimethylanilines and dimethylphenols yield in the one-pot reaction would be equal to or lower than the dimethylphenols yield in step 1. However, the results showed the opposite trend, where step 1 only generated 27.4% of dimethylphenols compared to 49.5% of the total dimethylanilines and dimethylphenols yield in the one-pot reaction. Given that the only difference between the one-pot reaction and step 1 is the presence of NH_3, it is clear that NH_3 has enhanced the hydrogenolysis of PPO.

We conducted a recycling test to assess the reusability of the 2% Pd_7Ru_3/CNT. The yield of dimethylanilines decreased after each run, reaching 7% at the third run (Fig. S10a†). Elemental analysis of the reaction mixture using ICP-OES indicated that the leaching of Pd and Ru from the catalyst was minimal, accounting for less than 0.2% (Fig. S10b†). Hence, metal leaching is unlikely to be the primary pathway for deactivation. Raman spectroscopy revealed no significant alteration in the I_D/I_G ratios of the catalysts after each run, implying the stability of the CNT support (Fig. S10c†). TEM analysis on the used catalyst revealed the aggregation of metal particles (Fig. S10d†), suggesting that metal aggregation may be the primary pathway for catalyst deactivation. These findings align with our observations regarding the impact of catalyst loading on product yields, where a smaller particle size was found to be more beneficial in terms of dimethylaniline yields (Fig. 2d and Fig. S3†).

Finally, we conducted a demonstration of isolating dimethylanilines from the product mixture. Successful separation was achieved through a straightforward procedure involving treatment with HCl and NaOH, followed by extraction

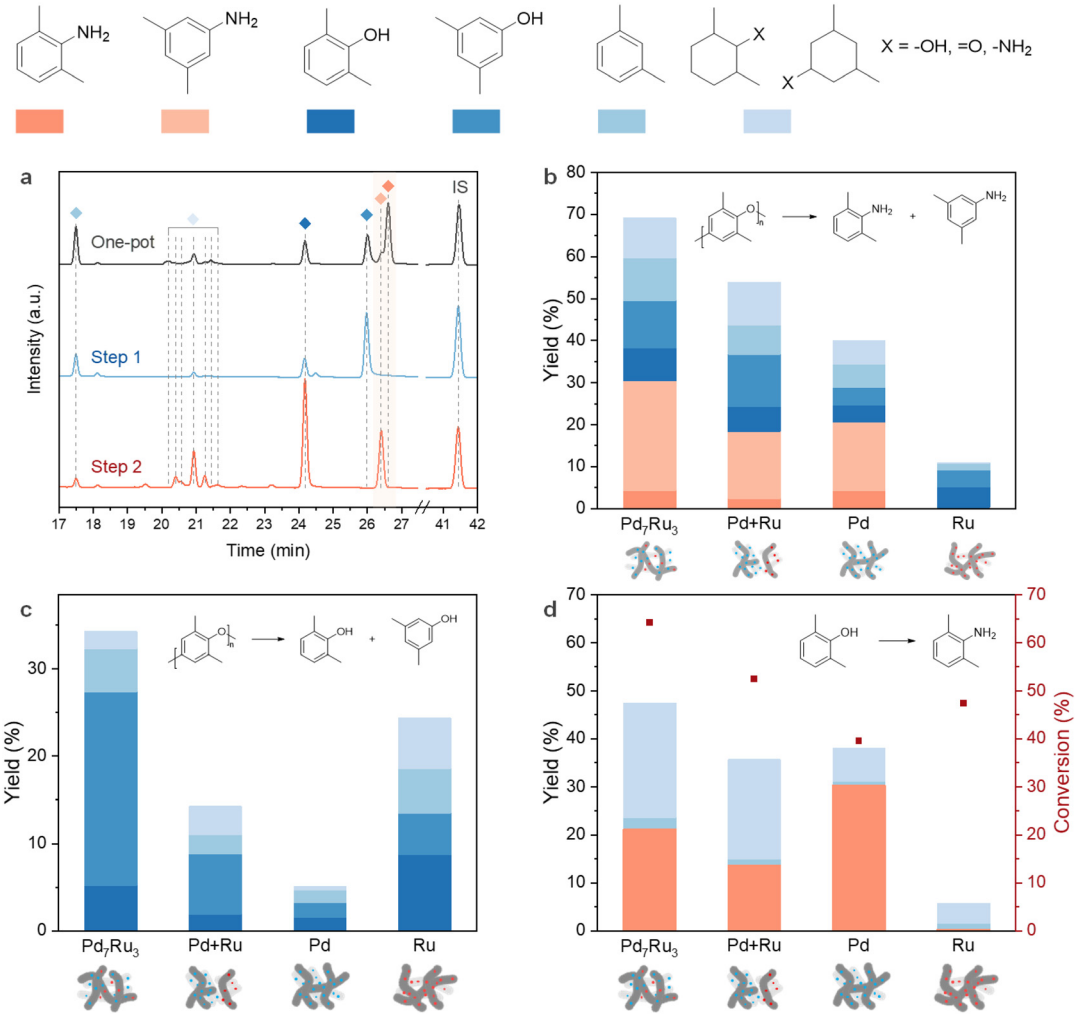

Fig. 5 (a) GC-FID chromatogram and products yield of (b) one-pot reaction, (c) Step 1 and (d) Step 2. Condition for one-pot reaction: 50 mg PPO, 50 mg catalyst (2 wt% metal loading), 4 mL octane, 1 mL NH_3 aqueous solution 25%, 5 bar H_2, 280 °C, 4 h. For step 1, 25% aqueous NH_3 solution was replaced by water. 2,6-dimethylphenol was used as starting material for Step 2. Pd + Ru: physical mixture of 2% Pd/CNT and 2% Ru/CNT at 7 : 3 weight ratio. IS: internal standard (pentadecane).

with ethyl acetate (Fig. S11†). This eliminates the necessity for column chromatography or distillation in isolating dimethylanilines.

Conclusion

In conclusion, we have developed a heterogeneous catalytic process using a 2% Pd_7Ru_3/CNT bimetallic catalyst for producing substituted anilines from PPO in an aqueous NH_3-octane mixture. This method yields primarily dimethylanilines (30%), accompanied by dimethylphenols (19%) and *m*-xylene (10%) in a one-pot amination. Based on the control experiments using deuterium and the kinetic studies, a reaction pathway from PPO to dimethylanilines involving hydrogenolysis, hydrogenation, imination and dehydrogenation steps was proposed. The synergy of Ru and Pd significantly enhances the dimethylanilines production in the one-pot transformation, particularly during the hydrogenolysis, whereas the amination relied dominantly on Pd. Notably, dimethylanilines can be isolated from the reaction mixture through a straightforward acid–base treatment and extraction, eliminating the need for column chromatography or distillation. This strategy not only leverages PPO waste for valuable product generation but also potentially diminishes the dependence on petroleum feedstocks for dimethylanilines synthesis.

Author contributions

N. Y. conceived and supervised the project. N. Y., G. G. and P. T. T. N. designed experiments. P. T. T. N. conducted experiments, catalyst synthesis and characterization. J. M. participated in some experiments. B. Y. and Q. H. conducted TEM analysis of catalysts. N. Y., G. G. and P. T. T. N. wrote the paper.

Conflicts of interest

There are no conflicts to declare.

Acknowledgements

We thank the NRF Investigatorship (NRF-NRFI07–2021–0006) for the financial support. We also thank Ms. Xiao Yiying for helping with Raman measurement, and Mr Li Xiran for helping with some experiments during the revision.

References

1 OECD, *Global Plastics Outlook*, 2022.
2 K. Ragaert, L. Delva and K. Van Geem, *Waste Manage.*, 2017, **69**, 24–58.
3 I. Vollmer, M. J. F. Jenks, M. C. P. Roelands, R. J. White, T. van Harmelen, P. de Wild, G. P. van der Laan, F. Meirer, J. T. F. Keurentjes and B. M. Weckhuysen, *Angew. Chem., Int. Ed.*, 2020, **59**, 15402–15423.
4 A. J. Martín, C. Mondelli, S. D. Jaydev and J. Pérez-Ramírez, *Chem*, 2021, **7**, 1487–1533.
5 J. E. Rorrer, A. M. Ebrahim, Y. Questell-Santiago, J. Zhu, C. Troyano-Valls, A. S. Asundi, A. E. Brenner, S. R. Bare, C. J. Tassone, G. T. Beckham and Y. Román-Leshkov, *ACS Catal.*, 2022, **12**, 13969–13979.
6 J. E. Rorrer, G. T. Beckham and Y. Román-Leshkov, *JACS Au*, 2021, **1**, 8–12.
7 P. A. Kots, S. Liu, B. C. Vance, C. Wang, J. D. Sheehan and D. G. Vlachos, *ACS Catal.*, 2021, **11**, 8104–8115.
8 J. E. Rorrer, C. Troyano-Valls, G. T. Beckham and Y. Román-Leshkov, *ACS Sustainable Chem. Eng.*, 2021, **9**, 11661–11666.
9 L. Chen, L. C. Meyer, L. Kovarik, D. Meira, X. I. Pereira-Hernandez, H. Shi, K. Khivantsev, O. Y. Gutiérrez and J. Szanyi, *ACS Catal.*, 2022, **12**, 4618–4627.
10 Y. Nakaji, M. Tamura, S. Miyaoka, S. Kumagai, M. Tanji, Y. Nakagawa, T. Yoshioka and K. Tomishige, *Appl. Catal., B*, 2021, **285**, 119805.
11 B. C. Vance, P. A. Kots, C. Wang, Z. R. Hinton, C. M. Quinn, T. H. Epps, L. T. J. Korley and D. G. Vlachos, *Appl. Catal., B*, 2021, **299**, 120483.
12 C. Wang, T. Xie, P. A. Kots, B. C. Vance, K. Yu, P. Kumar, J. Fu, S. Liu, G. Tsilomelekis, E. A. Stach, W. Zheng and D. G. Vlachos, *JACS Au*, 2021, **1**, 1422–1434.
13 M. Tamura, S. Miyaoka, Y. Nakaji, M. Tanji, S. Kumagai, Y. Nakagawa, T. Yoshioka and K. Tomishige, *Appl. Catal., B*, 2022, **318**, 121870.
14 S. Liu, P. A. Kots, B. C. Vance, A. Danielson and D. G. Vlachos, *Sci. Adv.*, 2021, **7**, eabf8283.
15 G. Zichittella, A. M. Ebrahim, J. Zhu, A. E. Brenner, G. Drake, G. T. Beckham, S. R. Bare, J. E. Rorrer and Y. Román-Leshkov, *JACS Au*, 2022, **2**, 2259–2268.
16 C. Jia, S. Xie, W. Zhang, N. N. Intan, J. Sampath, J. Pfaendtner and H. Lin, *Chem. Catal.*, 2021, **1**, 437–455.
17 S. D. Jaydev, A. J. Martín and J. Pérez-Ramírez, *ChemSusChem*, 2021, **14**, 1–8.
18 O. Akin, R. J. Varghese, A. Eschenbacher, J. Oenema, M. S. Abbas-Abadi, G. D. Stefanidis and K. M. Van Geem, *J. Anal. Appl. Pyrolysis*, 2023, **172**, 106036.
19 A. Eschenbacher, R. J. Varghese, E. Delikonstantis, O. Mynko, F. Goodarzi, K. Enemark-Rasmussen, J. Oenema, M. S. Abbas-Abadi, G. D. Stefanidis and K. M. Van Geem, *Appl. Catal., B*, 2022, **309**, 121251.
20 Y. Jing, Y. Wang, S. Furukawa, J. Xia, C. Sun, M. J. Hülsey, H. Wang, Y. Guo, X. Liu and N. Yan, *Angew. Chem., Int. Ed.*, 2021, **60**, 5527–5535.
21 S. Hongkailers, Y. Jing, Y. Wang, N. Hinchiranan and N. Yan, *ChemSusChem*, 2021, **14**, 4330–4339.
22 S. Lu, Y. Jing, B. Feng, Y. Guo, X. Liu and Y. Wang, *ChemSusChem*, 2021, **14**, 4242–4250.
23 F. Zhang, M. Zeng, R. D. Yappert, J. Sun, Y.-H. Lee, A. M. LaPointe, B. Peters, M. M. Abu-Omar and S. L. Scott, *Science*, 2020, **370**, 437–441.
24 R. Cao, M.-Q. Zhang, C. Hu, D. Xiao, M. Wang and D. Ma, *Nat. Commun.*, 2022, **13**, 4809.
25 Y. Li, M. Wang, X. Liu, C. Hu, D. Xiao and D. Ma, *Angew. Chem., Int. Ed.*, 2022, **61**, e202117205.
26 M. S. Lehnertz, J. B. Mensah and R. Palkovits, *Green Chem.*, 2022, **24**, 3957–3963.
27 X. Chen, S. Song, H. Li, G. Gözaydın and N. Yan, *Acc. Chem. Res.*, 2021, **54**, 1711–1722.
28 K. Lee, Y. Jing, Y. Wang and N. Yan, *Nat. Rev. Chem.*, 2022, **6**, 635–652.
29 A. B. Raheem, Z. Z. Noor, A. Hassan, M. K. A. Hamid, S. A. Samsudin and A. H. Sabeen, *J. Cleaner Prod.*, 2019, **225**, 1052–1064.
30 J. Demarteau, I. Olazabal, C. Jehanno and H. Sardon, *Polym. Chem.*, 2020, **11**, 4875–4882.
31 S. Ghorbantabar, M. Ghiass, N. Yaghobi and H. Bouhendi, *J. Mater. Cycles Waste Manage.*, 2021, **23**, 526–536.
32 A. P. More, S. R. Kokate, P. C. Rane and S. T. Mhaske, *Polym. Bull.*, 2017, **74**, 3269–3282.
33 N. D. Pingale and S. R. Shukla, *Eur. Polym. J.*, 2009, **45**, 2695–2700.
34 P. Gupta and S. Bhandari, in *Recycling of Polyethylene Terephthalate Bottles*, ed. S. Thomas, A. Rane, K. Kanny, A. V. K. and M. and G. Thomas, William Andrew Publishing, 2019, pp. 109–134, DOI: **10.1016/B978-0-12-811361-5.00006-7**.
35 R. Radadiya, S. Shahabuddin and R. Gaur, *J. Polym. Sci.*, 2023, **61**, 1241–1251.
36 W. Stuyck, K. Janssens, M. Denayer, F. De Schouwer, R. Coeck, K. V. Bernaerts, J. Vekeman, F. De Proft and D. E. De Vos, *Green Chem.*, 2022, **24**, 6923–6930.
37 R. Coeck, A. De Bruyne, T. Borremans, W. Stuyck and D. E. De Vos, *ACS Sustainable Chem. Eng.*, 2022, **10**, 3048–3056.
38 N. A. Stephenson, S. H. Gellman and S. S. Stahl, *RSC Adv.*, 2014, **4**, 46840–46843.

39 S. Tian, Y. Jiao, Z. Gao, Y. Xu, L. Fu, H. Fu, W. Zhou, C. Hu, G. Liu, M. Wang and D. Ma, *J. Am. Chem. Soc.*, 2021, **143**, 16358–16363.
40 J. Ma, D. Le and N. Yan, *Chem*, 2023, **9**(10), 2869–2880.
41 Polyphenylene Oxide Market Size, Share & Trends Analysis Report By Application (Electronic Components, Fluid Handling, Air Separation Membranes, Medical Instruments, Automotive), And Segment Forecasts, 2020–2025, **https://www.grandviewresearch.com/industry-analysis/polyphenylene-oxide-ppo-market**, (accessed June 2023).
42 Y. Jing, Y. Wang, S. Furukawa, J. Xia, C. Sun, M. J. Hulsey, H. Wang, Y. Guo, X. Liu and N. Yan, *Angew. Chem., Int. Ed.*, 2021, **60**, 5527–5535.
43 B. Feng, Y. Jing, Y. Guo, X. Liu and Y. Wang, *Green Chem.*, 2021, **23**, 9640–9645.
44 M. Meyer, in *Ullmann's Encyclopedia of Industrial Chemistry*, 2000, DOI: **10.1002/14356007.a28_455**.
45 *US Pat*, 3931298, 1976.
46 *US Pat*, 4188341, 1980.
47 *US Pat*, 4496763, 1985.
48 *DE Pat*, 1933636A1, 1969.
49 Global Industrial Grade 2,6-Dimethylaniline Market 2023 by Manufacturers, Regions, Type and Application, Forecast to 2029, **https://www.marketresearchreports.com/gir/global-industrial-grade-26-dimethylaniline-market-2023-manufacturers-regions-type-and**, (accessed June 2023).
50 Global 3,5-Dimethylaniline Market 2023 by Manufacturers, Regions, Type and Application, Forecast to 2029, **https://www.marketresearchreports.com/gir/global-35-dimethylaniline-market-2023-manufacturers-regions-type-and-application-forecast-2029**, (accessed June 2023).
51 K. Chen, Q. K. Kang, Y. Li, W. Q. Wu, H. Zhu and H. Shi, *J. Am. Chem. Soc.*, 2022, **144**, 1144–1151.
52 H. Hideaki, Y. Makoto, K. Yasushi, M. Takehiko and W. Katsuhiko, *Bull. Chem. Soc. Jpn.*, 1985, **58**, 1551–1555.
53 Y. Koizumi, X. Jin, T. Yatabe, R. Miyazaki, J. Y. Hasegawa, K. Nozaki, N. Mizuno and K. Yamaguchi, *Angew. Chem., Int. Ed.*, 2019, **58**, 10893–10897.
54 X. Liu, W. Chen, J. Zou, L. Ye and Y. Yuan, *ACS Sustainable Chem. Eng.*, 2022, **10**, 6988–6998.
55 Y. Ono and H. Ishida, *J. Catal.*, 1981, **72**, 121–128.
56 J. Zhang, Q. Jiang, D. Yang, X. Zhao, Y. Dong and R. Liu, *Chem. Sci.*, 2015, **6**, 4674–4680.
57 N. F. Dummer, S. Bawaked, J. Hayward, R. Jenkins and G. J. Hutchings, *Catal. Today*, 2010, **154**, 2–6.
58 Y. Wang, S. Furukawa, S. Song, Q. He, H. Asakura and N. Yan, *Angew. Chem., Int. Ed.*, 2020, **59**, 2289–2293.
59 W. Deng, Y. Wang, S. Zhang, K. M. Gupta, M. J. Hulsey, H. Asakura, L. Liu, Y. Han, E. M. Karp, G. T. Beckham, P. J. Dyson, J. Jiang, T. Tanaka, Y. Wang and N. Yan, *Proc. Natl. Acad. Sci. U. S. A.*, 2018, **115**, 5093–5098.
60 Y. Wang, S. Furukawa, X. Fu and N. Yan, *ACS Catal.*, 2019, **10**, 311–335.
61 Y. Xiao, C. W. Lim, J. Chang, Q. Yuan, L. Wang and N. Yan, *Green Chem.*, 2023, **25**, 3117–3126.
62 G. M. Bhalerao, A. K. Sinha and V. Sathe, *Phys. E*, 2008, **41**, 54–59.
63 X. Li and Y. Xiang, *Sci. China, Ser. B: Chem.*, 2007, **50**, 746–753.
64 U. Sanyal, Y. Song, N. Singh, J. L. Fulton, J. Herranz, A. Jentys, O. Y. Gutiérrez and J. A. Lercher, *ChemCatChem*, 2019, **11**, 575–582.
65 Y. Rong, N. Ji, Z. Yu, X. Diao, H. Li, Y. Lei, X. Lu and A. Fukuoka, *Green Chem.*, 2021, **23**, 6761–6788.
66 E. Paone, A. Beneduci, G. A. Corrente, A. Malara and F. Mauriello, *Mol. Catal.*, 2020, **497**, 111228.
67 M. Zhao, L. Zhao, J.-P. Cao, W. Jiang, J.-X. Xie, C. Zhu, S.-Y. Wang, Y.-L. Wei, X.-Y. Zhao and H.-C. Bai, *Chem. Eng. J.*, 2022, **435**, 134911.
68 Q. Fu, F. Xin, X. Yin, Y. Song and Y. Xu, *Int. J. Hydrogen Energy*, 2021, **46**, 22446–22453.
69 E. Levernier, K. Tatoueix, S. Garcia-Argote, V. Pfeifer, R. Kiesling, E. Gravel, S. Feuillastre and G. Pieters, *JACS Au*, 2022, **2**, 801–808.
70 NIST Chemistry WebBook, SRD 69, webbook.nist.gov, (accessed Sep 2023).
71 *US Pat*, 3931298, 1976.
72 T. Cuypers, P. Tomkins and D. E. De Vos, *Catal. Sci. Technol.*, 2018, **8**, 2519–2523.
73 T. Li, H. Lin, X. Ouyang, X. Qiu, Z. Wan and T. Ruan, *Fuel*, 2020, **278**, 118324.